Resistive switching and threshold switching behaviors in La$_{0.1}$Bi$_{0.9}$Fe$_{1-x}$Co$_x$O$_3$ ceramics

S. Y. Wang,[1,a)] W. F. Liu,[2,a)] J. Gao,[3] Xue Qiu,[1] Yu Feng,[1] X. G. Hou,[1] D. S. Yu,[1] and D. J. Li[1]

[1]*College of Physics and Electronic Information Science, Tianjin Normal University, Tianjin 300074, China*
[2]*Tianjin Key laboratory of Low Dimensional Materials Physics and Preparing Technology, Faculty of Science, Tianjin University, Tianjin 300072, China*
[3]*Department of Physics, the University of Hong Kong, Pokfulam Road, Hong Kong*

The effects of cobalt doping on the electrical conductivity of La$_{0.1}$Bi$_{0.9}$Fe$_{1-x}$Co$_x$O$_3$ (LBFCO, x = 0, 0.01, 0.03) ceramics were investigated. It is found that the leakage current increases with cobalt dopant concentration in LBFCO. On the application of bias voltage LBFCO ceramics with cobalt doping exhibits resistive switching effects at room temperature and threshold switching effects at elevated temperatures (50 °C and 80 °C). X-ray photoelectron spectroscopy of LBFCO ceramics show that cobalt dopant is bivalent as an acceptor, which induces an enhancement of oxygen vacancy concentration in LBFCO ceramics. Possible mechanisms for both resistive switching and threshold switching effects are discussed on the basis of the interplay of bound ferroelectric charges and mobile charged defects. © *2012 American Institute of Physics.* [http://dx.doi.org/10.1063/1.4743013]

I. INTRODUCTION

Reversible resistive switching (RS) behaviors have been extensively investigated in recent years, due to their potential applications in nonvolatile resistance random access memory (RRAM) devices.[1] RRAM have been demonstrated to possess advantages such as low-power consumption, high-speed operation, and high-density integration. Many transition metal oxides were found to exhibit the RS behavior. Furthermore, RS was also observed in oxides with perovskite structure, such as Pb(Zr,Ti)O$_3$ and BiFeO$_3$ (BFO).[2–6] Therein, BFO is one of the most actively studied materials, due to its multiferroic properties and potential in applications of memory and magnetoelectric devices.[2–6] Regarding its electric conduction, the containing of transition metal with unpaired *d* electron results in a relatively small optical gap and gives rise to a high concentration of charged impurities and defects. It is reported that a metal-insulator transition could be induced by hydrostatic pressure in single crystals of BFO.[7] Moreover, the variation of optical band gap and conductivity at domain walls were also observed in BFO films,[8] which indicates the possibility to stabilize some conducting sates in those multiferroic ceramics.

Recently, Yang *et al.* reported the observation of a resistive switching behavior in capacitors comprised of Ca-doped BFO films and SrRuO$_3$ electrodes, which was attributed to the doping-driven competition between energetically conducting and insulating ground states.[3] RS behaviors were also found in Pt/BFO/SrRuO$_3$ capacitors, but they have been ascribed to the polarization modulated barriers height at both electrode/ferroelectric interfaces.[2,4] Moreover, based on a certain type of defects (ionic or electronic) mediated conduction mechanisms, unipolar[9] and bipolar[5,10] resistive switch-

ing behaviors were reported in pure or doped BFO thin films. Furthermore, it was reported that when the electric polarization is flipped by an external voltage, the electric conduction in bulk BFO crystals is highly nonlinear and unidirectional, showing RS behaviors upon polarization reversal.[5] However, up until now, the possibility to induce RS effect in polycrystalline BFO ceramics has never been considered. Actually, the switchable diode effect has been rarely reported in BFO ceramics and the mechanism behind the switchable diode effect remains unclear.

In this paper, we present the experimental results of reversible RS behaviors observed in La$_{0.1}$Bi$_{0.9}$Fe$_{1-x}$Co$_x$O$_3$ (x = 0, 0.01, 0.03) ceramics. We found that the electrical conductivity of ceramics of composition La$_{0.1}$Bi$_{0.9}$Fe$_{1-x}$Co$_x$O$_3$ increases with Co dopant concentration and they exhibit RS effects on application of dc bias voltage. The mechanism for the observed doping-driven modulation of resistivity was discussed, based on the electronic structures of ceramics by x-ray photoelectron spectroscopy (XPS) investigation.

II. EXPERIMENT

The La$_{0.1}$Bi$_{0.9}$FeO$_3$ (LBFO), 1% Co-doped LBFO (La$_{0.1}$Bi$_{0.9}$Fe$_{0.99}$Co$_{0.01}$O$_3$, LBFCO1), and 3% Co-doped LBFO (La$_{0.1}$Bi$_{0.9}$Fe$_{0.97}$Co$_{0.03}$O$_3$, LBFCO3) ceramics were prepared by a modified rapid sintering process (MRSP). Detailed description for synthesis can be found elsewhere.[11] The phase analysis crystalline structure of the ceramic samples was examined by x-ray diffraction (XRD, Rigaku D-max 2500 PC) using Cu K$_\alpha$ radiation. For the measurement of electrical properties, these ceramic discs were polished and coated with silver paste on both sides as electrodes to form the capacitor structure. Ferroelectric polarization and leakage current versus electric field (J-E) were measured with an Aixacct model TF 2000 ferroelectric device analyzer. In order to minimize the influence of the polarization of charge carrier on the leakage current data, a relatively

a)Authors to whom correspondence should be addressed. Electronic addresses: shouyu.wang@yahoo.com and wfliu26@tju.edu.cn. Tel./Fax: +86-23766503.
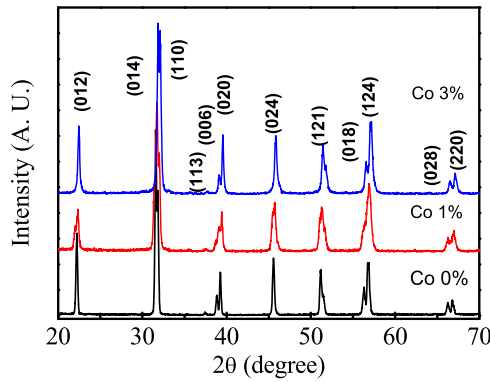
FIG. 1. XRD patterns of $La_{0.1}Bi_{0.9}Fe_{1-x}Co_xO_3$ (x = 0, 0.01, 0.03) ceramics.

long delay time of 5 s was used, i.e., the current measurement was performed after each application of bias voltages for 5 s. The valence state of elements was examined by x-ray photoelectron spectroscopy (ESCALab220i-XL) using 300 W Al$K\alpha$ (1486.6 eV) radiation.

III. RESULTS AND DISCUSSION

The XRD patterns of the ceramics were shown in Fig. 1. The indexed Bragg reflections show no traces of impurity phases in all ceramic samples. All XRD profiles show split reflections at $2\theta = 39.5°$ and $57.2°$. This indicates that as cobalt doping up to 3 at. % at Fe site, the rhombohedral structure of LBFO does not change appreciably, except a minor upward shift of peak position. It has been indicated that single phase material can be obtained for x < 0.36 in $BiCo_xFe_{1-x}O_3$.[12] Furthermore, the XRD data were detailed analyzed by Rietveld refinement method, considering that the samples have rhombohedrally distorted perovskite structure with R3c space group.[13] The lattice parameters are refined as $a = b = 5.5804$ Å, 5.5752 Å, and 5.5739 Å, c = 13.8290 Å, 13.8257 Å, and

13.8244 Å for LBFO, LBFCO1, and LBFCO3 ceramics, respectively. We can see that the lattice parameters are decreasing with cobalt concentration. It is calculated that for increasing the cobalt concentration, there is a gradual shrinkage in unit cell volume of ceramics from 372.87 Å^3 to 372.26 and 371.96 Å^3. This could be ascribed to the smaller ionic radius of cobalt (Co^{3+}, 0.63 Å and Co^{2+}, 0.74 Å) than that of ion (Fe^{3+}, 0.64 Å and Fe^{2+}, 0.76 Å),[14] which clearly confirms that the cobalt is successfully doped in the lattice of LBFO ceramics.

J-E characteristics with the linear scales in the bias range of ± 10 kV/cm are shown in Fig. 2(a) for all samples. It can be seen that Co doping has a strong influence on the electric properties of the LBFCO ceramics. With increasing Co doping concentration, the J is enhanced dramatically. Figs. 2(b)–2(d) show the J-E curves for LBFCO ceramics in the bias range of ± 150 kV/cm. The J exhibits a nonlinear relationship with E at higher bias region and it shows strong dependence on the scanning direction of E. In measurement process, the bias voltage was swept from $0 \rightarrow 150 \rightarrow 0 \rightarrow -150 \rightarrow 0$ kV/cm with a step of 1 kV/cm. As the cobalt concentration is increased, there is an obvious enhancement in J values. Similar results have also been reported in acceptor ions doped $BiFeO_3$ ceramics and thin films.[3] Moreover, for increasing cobalt doping concentration, the J-E curves show more and more distinct hysteresis behaviors, indicating that cobalt doping results in a RS effect in LBFCO ceramics.

As reported in our recent work,[11] LBFO ceramics synthesized with MRSP method has high resistances, which guarantees the observation of saturated polarization loops and switching current at room temperature. Hence, in highly resistive LBFO ceramics, the current hysteresis is small enough to be ignored (Fig. 2(a)). However, in LBFCO ceramics with cobalt doping, the leakage current shows profound distinct hysteresis behavior, as shown in Fig. 2(d). When the E is swept from $0 \rightarrow 150$ kV/cm, the leakage current significantly
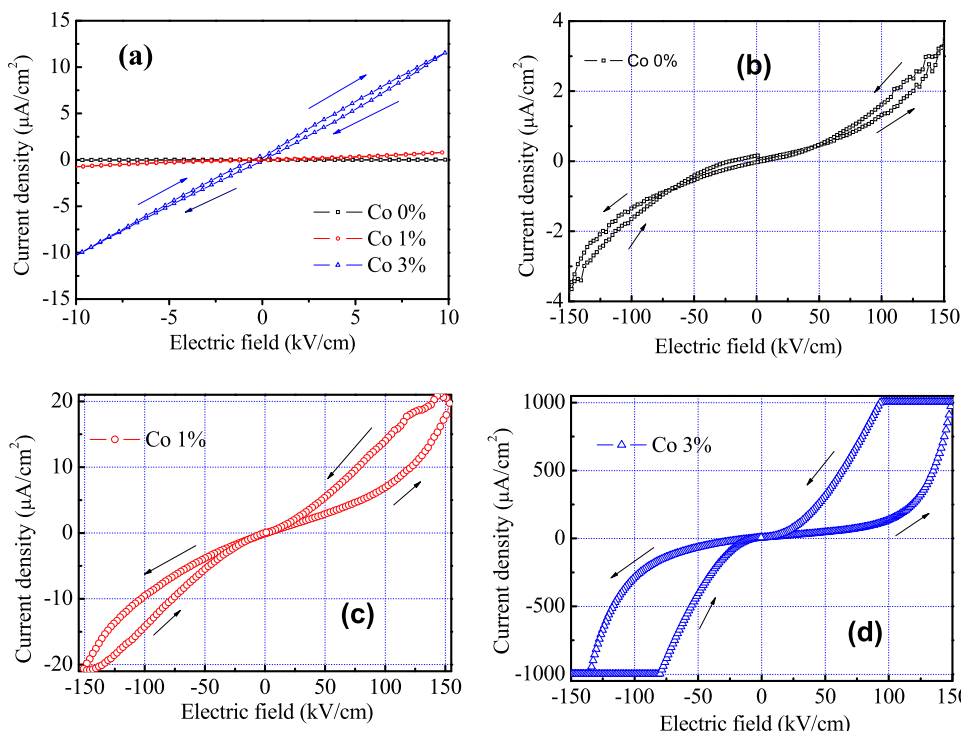

FIG. 2. (a) J-E characteristics in the bias range of ± 10 kV/cm for LBFO ceramics with various Co concentrations. J-E curves in the bias range of ± 150 kV/cm for (b) LBFO, (c) LBFCO1, and (d) LBFCO3 ceramics.

increases following a nonlinear feature after $\sim$100 kV/cm and reaches a compliance value of 1000 μA/cm^2 at $\sim$150 kV/cm. After reversing the electric field (150 $\rightarrow$ 0 kV/cm), the leakage current exhibits higher values than those in forward scanning process, resulting in current loops. In negative bias region, similar hysteresis loop also exists in J-E curves for Co-doped LBFO ceramics. When the maximum driving electric field E decreases, the hysteresis loop becomes smaller.[15]

The ferroelectric properties were characterized by probing the ferroelectric polarization and displacement current versus electric filed (P-E, I$_d$-E) of LBFCO ceramics. In order to preclude leakage current effect, switching current were measured at high frequencies. Typical P-E and I$_d$-E curves at 1 kHz, shown in Fig. 3, were measured on a 0.4-mm-thick LBFCO3 ceramic sandwiched with Ag electrodes at room temperature. The clear peaks in I$_d$-E curve confirm the presence of intrinsic ferroelectricity. With the maximum electric field of 150 kV/cm, the remnant polarization of $\sim$11 μC/cm^2 was observed with a coercive field (E_c) of 79 kV/cm.

In J-E curves shown in Figs. 2(b)–2(d), the magnitude of E is larger than the value E_c of LBFCO. Hence, during the sweeping process of E, the ferroelectric domains would be aligned, accompanying with RS behaviors in Ag/LBFCO/Ag capacitor. This indicates that the conductive states of LBFCO ceramics correlates with the direction of ferroelectric polarization. To examine the influences of polarization reversal on the electric conductivity of capacitor, a positively (or negatively) poling pulse (6 kV, 10 ms) was applied to the top Ag electrode to polarize the Ag/LBFCO3/Ag into P$_r^+$ (or Pr-) states. After turning off the poling E, the J-E curves were measured. Fig. 3(b) shows the *J-E* curves for P$_r^+$ and P$_r^-$ states for Ag/LBFCO3/Ag capacitors at room temperature. The currents in P$_r^+$ state with solid circle symbols increases exponentially with positive voltage but increases slowly with negative one, indicating a forward diode-like rectifying characteristic, whereas for the P$_r^-$ state, the J

exhibits a reverse diode-like behavior. As shown in Fig. 3(b), when the direction of ferroelectric polarization is the same to that of leakage current, the J exhibits large values. The similar diode-like conduction phenomena have also been observed for a variety of ferroelectric materials, including single crystals and thin films of BiFeO$_3$.[2–4] For a typical p-n junction diode, the forward current density follows an exponential relationship with bias voltage formulated by

$$J = A \exp \frac{qV}{\alpha k_B T}, \tag{1}$$

where q is the electron charge, V is bias voltage, α is a constant called the ideality factor, and k_B is the Boltzmann constant. The rectification ratios defined as the ratios of the positive current divided by the negative one at $\pm$75 kV/cm are 5.1, and 13.6 for P$_r^+$ and P$_r^-$ states, respectively.

The E dependence of current density is highly non-linear, and there exists a significant asymmetry with respect to the polarity of E. This asymmetric electronic transport nature with symmetric Ag electrodes indicates that the observed resistive switching behaviors are governed by the bulk characteristics of LBFCO ceramics. In order to understand electronic transport mechanism in LBFCO capacitors, we investigated the detailed electric field dependence of current density with symmetric Ag electrodes. The possible conduction mechanisms including the interface-limited Schottky emission, bulk-limited Poole-Frenkel (PF) emission, and space-charge-limited current (SCLC) conduction were examined for the observed J-E curves.[11] It appears that the bulk-limited SCLC mechanism is the dominant conduction route, rather than the Schottky or PF emission, as indicated by the power-law relations shown in the Fig. 3(c). On the other hand, in resistive switching effect, the rectification direction switches when electric polarization is flipped by large external voltage pulse, proving that the RS effect is associated with the bulk
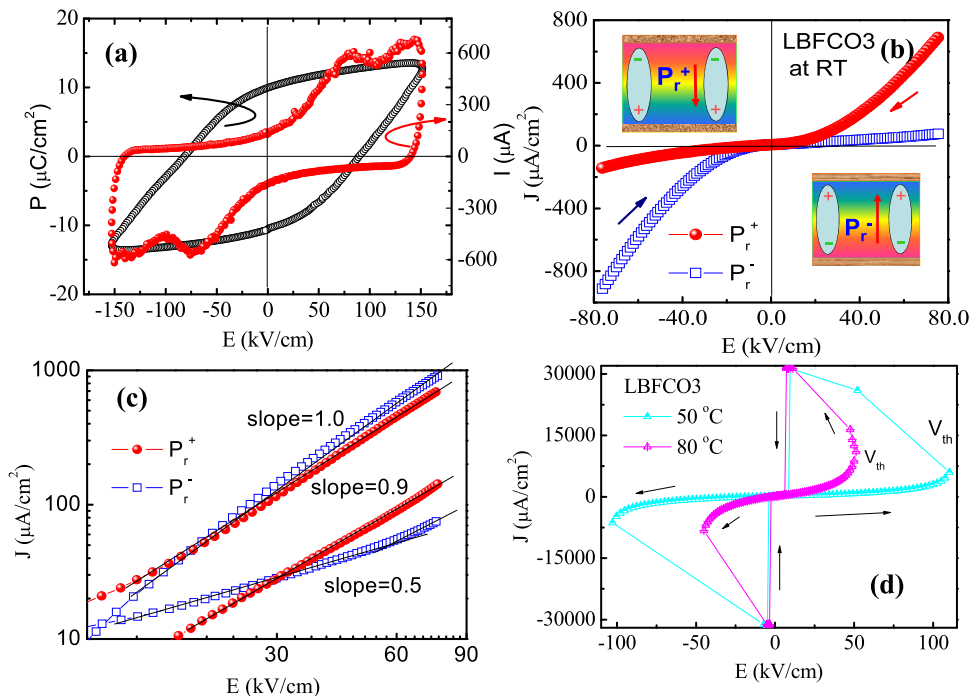

FIG. 3. (a) Typical ferroelectric hysteresis loop and displacement current of LBFCO3 ceramics under the frequency of 1 kHz at room temperature; J-E curves (b) in linear scale and (c) log scale for LBFCO3 ceramics measured at the bias voltage of $\pm$75 kV/cm in P$_r^+$ and P$_r^-$ states at room temperature, which indicates the forward and reverse diode-like characteristics; (d) at 50 °C and 80 °C, J-E curves for LBFCO3 ceramics exhibit threshold switching behaviors.

properties of LBFCO ceramics. Furthermore, we examined the influence of an asymmetric configuration with *Ag* and *In* electrodes on the electronic transport properties of LBFCO ceramics. Although Ag and In have different work functions (4.3 eV for Ag and 3.8 eV for In), *J-E* characteristics are almost identical to the configuration with symmetric Ag electrodes, irrespective of the type of electrode. All of these observations indicate that the diode effect and resistive switching behavior stems primarily from the bulk characteristics of LBFCO, rather than an interfacial effect.

The *J-E* curves of LBFCO3 were also investigated at elevated temperatures. It is found that the *J* increases drastically with temperature from room temperature to 80 °C. The most intriguing phenomenon is a symmetric threshold switching (TS) behavior at a higher temperature instead of the asymmetric diode-like characteristics. Fig. 3(d) shows the typical J-E curves measured at 50 °C and 80 °C. In J-E curve probed at 50 °C, in scanning range from $0 \rightarrow 110$ kV/cm, the J increases with the applied voltage, which is in the "off" state. This state can be divided into three parts, a linear part ($0 \rightarrow 85$ kV/cm), a second part ($85 \rightarrow 100$ kV/cm) following the Poole-Frenkel relation,[16] and a third part ($100 \rightarrow 110$ kV/cm) with exponentially increase of current. After threshold voltage (V_{th}) $\sim$110 kV/cm, the further increase in the E switches the capacitor to an "on" state. In "on" state, a reducing of bias voltage results in a returning of current to zero. Similar TS behaviors are also observed in J-E curves of 80 °C except the higher current density and smaller V_{th} values.

It is well known that TS is the result of a negative differential resistance (NDR) behavior, which appears as a sudden transition to a highly conductive state, once the applied electrical field exceeds a critical voltage. It is reported that the TS phenomenon has been observed in amorphous Sb_xSe_{1-x},[16] chalcogenide glasses $Ge_2Sb_2Te_5$,[17] and NbO_x (Ref. 18) films. The TS behaviors were ascribed to the reversible phase change between the amorphous and crystalline states induced by Joule heating.[19] In this study, the TS behaviors were observed in polycrystalline LBFCO ceramics at elevated temperatures, which may be related to high-density mobile charges in polycrystalline ceramics. In order to investigate the electronic structures of LBFCO, the valence band and core levels of elements in LBCFO ceramics were studied by XPS.

Fig. 4(b) shows the XPS spectra of O 1s core level of LBFO and LBFCO3 ceramics. For LBFCO3, one of two peaks is located at a lower binding energy of 529.88 eV, which shifts 0.60 eV towards the high binding energy compared to that of LBFO. The other peak in O 1s core level line is located at 531.76 eV. In LBFCO3 ceramics, the two peaks may correspond to two types of oxygen atoms. The former (O_F) can be attributed to the main peak of oxygen atoms in the LBFCO ceramic, while the latter (O_L) is related to the presence of oxygen vacancy.[20] Comparing the ratio of the fitted peak areas, concentration ratios of O_F and O_L in the LBFO and LBFCO3 ceramics are 87:13 and 51:49, respectively. This indicates that Co dopant results in an increase of oxygen vacancy concentration in LBFCO ceramics.

Fig. 4(a) shows the XPS spectrum of Co2p core level of LBFCO3 ceramics. The $Co2p_{3/2}$ binding energy is located as 780.4 eV, which is inconsistent with the previously reports,
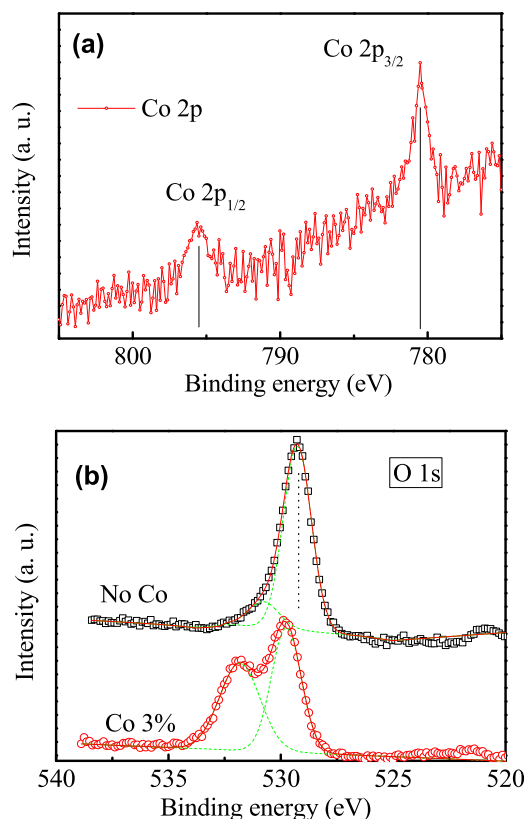

FIG. 4. XPS spectrum for (a) Co2p and (b) O1s core levels for LBFO and LBFCO3 ceramics.

i.e., the binding energy is comparable to that of the energy of corresponding photoelectrons of Co^{2+} in CoO.[21] Therefore, the XPS results demonstrate that the cobalt in LBFCO3 ceramics is in the +2 valence state and plays a role of an acceptor, which stimulates the formation of oxygen vacancies by the reaction

$$2Co_2O_3 \Rightarrow 4Co_{Fe}^- + 3O_2[\text{volatization}] + 2V_O^{2+}. \quad (2)$$
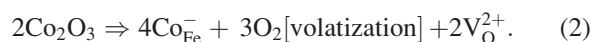
Consequently, the cobalt doping leads to an enhancement of oxygen vacancies concentration. The XPS valence band spectra show that the positions of the valence-band top is shifted to higher binding energy by $\sim$0.6 eV in LBFCO3 ceramics, demonstrating a shift of Fermi level (E_f) to higher values.[15] The similar effect was observed in Ca-doped $BiFeO_3$ films,[3] i.e., the concentration of oxygen vacancies modulate the energy position of E_f and thus modulates their resistivity.

In LBFCO, under the high electric field, a neutral oxygen vacancy (V_O) acting as donors may also release one or two electrons to become positively oxygen vacancies ($V_O^\bullet$ or $V_O^{\bullet\bullet}$). In P_r^+ state (Fig. 5(a)), under the influence of ferroelectric domain movement and polarization reversal, the released electrons would move and pile up near the bottom surface, while the positively $V_O^\bullet$ or $V_O^{\bullet\bullet}$ would accumulate near the top electrode. As a result, the positive oxygen vacancies and negative ions are locally unbalanced, forming a p-n junction like diode in Ag/LBFCO/Ag capacitor. This p-n junction would lead to the diode-like *J-E* curves. Via applying the opposite electric field, the ferroelectric polarization could be
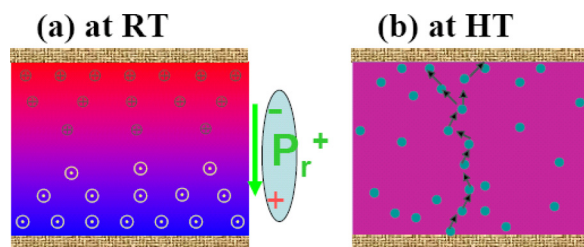
FIG. 5. A schematic diagram to show the formation of (a) a p-n junction like diode at room temperature (RT) and (b) the conducting filaments with oxygen vacancies and traps at high temperature (HT) in Ag/LBFCO/Ag capacitor.

reversed, accompanying with the redistribution of the mobile charged carriers in the capacitor, which results in the formation of reverse diode-like *J-E* curves. However, at elevated temperature, the mobility of the oxygen vacancies and charged defects is enhanced. With increasing applied voltage, the mobile charged carriers, including oxygen vacancies and traps, are able to align and form conducting paths as shown in Fig. 5(b), which are called conducting filaments in the filamentary mechanism.[9] Due to the negatively temperature dependent resistance effect, the high current flowing through the conducting filaments generates more heat. After the bias voltage beyond V_{th}, this eventually leads to a switch to the low-resistance state with large current density. As decreasing the applied voltage, the leakage current decreases dramatically and eventually return to the initial state.

IV. CONCLUSIONS

In summary, we report a resistive switching and a threshold switching effect upon the application of an electrical field. Both behaviors are a bulk effect rather than interface effect. The Co^{2+} ions dopant gives rise to high concentration of oxygen vacancies. As a result, the distribution of mobile charges is locally unbalanced upon application of electrical fields, which was thought as the reason for the observed resistive switching and asymmetric *J-E* curves.

ACKNOWLEDGMENTS

[1]J. Choi, J.-S. Kim, I. Hwang, S. Hong, I.-S. Byun, S.-W. Lee, S.-O. Kang, and B. H. Park, Appl. Phys. Lett. **96**, 262113 (2010).
[2]A. Q. Jiang, C. Wang, K. J. Jin, X. B. Liu, J. F. Scott, C. S. Hwang, T. A. Tang, H. B. Lu, and G. Z. Yang, Adv. Mater. **23**, 1277 (2011).
[3]C. H. Yang, J. Seidel, S. Y. Kim, P. B. Rossen, P. Yu, M. Gajek, Y. H. Chu, L. W. Martin, M. B. Holcomb, Q. He, P. Maksymovych, N. Balke, S. V. Kalinin, A. P. Baddorf, S. R. Basu, M. L. Scullin, and R. Ramesh, Nature Mater. **8**, 485 (2009).
[4]C. Wang, K.-J. Jin, Z.-T. Xu, L. Wang, C. Ge, H.-B. Lu, H.-Z. Guo, M. He, and G.-Z. Yang, Appl. Phys. Lett. **98**, 192901 (2011).
[5]K. Yin, M. Li, Y. Liu, C. He, Z. Fei, B. Chen, W. Li, X. Pan, and R.-W. Li, Appl. Phys. Lett. **97**, 042101 (2010).
[6]T. Choi, S. Lee, Y. J. Choi, V. Kiryukhin, and S.-W. Cheong, Science **324**, 63 (2009).
[7]A. G. Gavriliuk, V. V. Struzhkin, I. S. Lyubutin, S. G. Ovchinnikov, M. Y. Hu, and P. Chow, Phys. Rev. B **77**, 155112 (2008).
[8]J. Seidel, L. W. Martin, Q. He, Q. Zhan, Y.-H. Chu, A. Rother, M. E. Hawkridge, P. Maksymovych, P. Yu, M. Gajek, N. Balke, S. V. Kalinin, S. Gemming, F. Wang, G. Catalan, J. F. Scott, N. A. Spaldin, J. Orenstein, and R. Ramesh, Nature Mater. **8**, 229 (2009).
[9]S.-W. Chen and J.-M. Wu, Thin Solid Films **519**, 499 (2010).
[10]Y. Shuai, S. Zhou, D. Burger, M. Helm, and H. Schmidt, J. Appl. Phys. **109**, 124117 (2011).
[11]S. Y. Wang, X. Qiu, J. Gao, Y. Feng, W. N. Su, J. X. Zheng, D. S. Yu, and D. J. Li, Appl. Phys. Lett. **98**, 152902 (2011).
[12]S. Vasudevan and C. N. R. Rao, Mater. Res. Bull. **14**, 451 (1979).
[13]D. Lebeugle, D. Colson, A. Forget, M. Viret, P. Bonville, J. F. Marucco, and S. Fusil, Phys. Rev. B **76**, 024116 (2007).
[14]R. Haumon, I. A. Kornev, S. Lisenkov, L. bellaiche, J. Kreisel, and B. Dkhil, Phys. Rev. B **78**, 134108 (2008).
[15]S. Y. Wang, W. F. Liu, J. Gao, X. Qiu, Y. Feng, D. S. Yu, and D. J. Li, "Effects of cobalt doping on the electric properties of $La_{0.1}Bi_{0.9}FeO_3$ ceramics" (submitted).
[16]E. H. Aly and A. M. Ibrahim, J. Phys. D: Appl. Phys. **33**, 2549 (2000).
[17]S. W. Ryu, J. H. Lee, Y. B. Ahn, C. H. Kim, B. S. Yang, G. H. Kim, S. G. Kim, S.-H. Lee, C. S. Hwang, and D. J. Kim, Appl. Phys. Lett. **95**, 112110 (2009).
[18]J. Bae, I. Hwang, Y. Jeong, S.-O. Kang, S. Hong, J. Son, J. Choi, J. Kim, J. Park, M.-J. Seong, Q. Jia, and B. H. Park, Appl. Phys. Lett. **100**, 062902 (2012).
[19]S. R. Ovshinsky, Phys. Rev. Lett. **21**, 1450 (1968).
[20]J. F. Moulder, W. F. Stickle, P. E. Sobol, and K. D. Bomben, *Handbook of X-Ray Photoelectron Spectroscopy* (Perkin-Elmer Corporation, Minnesota, 1992).
[21]H.-J. Lee, S.-Y. Jeong, C. R. Cho, and C. H. Park, Appl. Phys. Lett. **81**, 4020 (2002).